The 15th International Symposium on Magnetic Bearings, August 3-6, 2016, Mojiko Hotel, Kitakyushu, Japan

ISMB15

Evaluation of Motor Losses and Efficiency in a d-q Axis Current Control Bearingless Motor

Masahide OOSHIMA* and Yuto GOMI*

*Department of Electrical and Electronic Engineering, Tokyo University of Science, Suwa

5000-1 Toyohira, Chino, Nagano 391-0292, Japan

Abstract

This paper presents the motor characteristic, for example, motor efficiency and losses, of a d-q axis current control bearingless motor, which has been proposed by the authors. In the d-q axis current control bearingless motor, both the motor drive and magnetic suspension can be successfully performed by one kind of stator winding. The torque and magnetic suspension characteristics have been found and the superiority of them is recognized. In this paper, the motor characteristic is derived by Finite Element (FE) analysis using a simulation software, and furthermore compared with those of the computed results of the conventional bearingless motors, which two kinds of windings for motor drive and magnetic suspension are wound in a stator core. Three types of the conventional bearingless motor with n-pole motor winding and $(n \pm 2)$-pole suspension winding are taken up in this paper. The stator and rotor iron losses, eddy current loss in the rotor permanent magnets are simulated, respectively. The motor efficiency is also estimated based on the computed output power and motor losses by FE analysis. The efficiency and loss in each part are compared with those of the conventional bearingless motors, respectively, and it is discussed in detail by what the difference of losses between the bearingless motor types is mainly caused.

Keywords : Magnetic bearing, Bearingless motor, Permanent magnet synchronous motor, Field-weakening control, Field-strengthening control, Losses and efficiency, Finite Element Method

1. Introduction

Recently, the bearingless motors (BELMs) are receiving attention as one of the drive systems under some special conditions, particularly, for high vacuum, aerospace and the other environment where the lubrication oil cannot be used due to some of its advantageous features as compared to the conventional motor drives. In the BELMs as there are no mechanical bearings, it is maintenance free and hence the longevity of the motor is increasing. The functions of motor and magnetic rotor levitation are successfully integrated so that the rotor shaft can be made shorter and at the same time it requires less number of inverters, controller and electric wires as compared to an electric motor with magnetic bearings. Thus, the overall size and cost of the bearingless machine is considerably reduced as compared to the machine with magnetic bearings. Furthermore, as the rotor shaft is shorter, there is no fear to decrease the critical speed of the BELM by the rotational axis bend.

The authors have proposed a d-q axis current control BELM, in which both the motor drive and magnetic suspension are successfully performed by one kind of the stator winding. The advantageous features of the proposed BELM are as follows. 1)The motor structure is just the same as the conventional brushless dc motors. The stator winding is short-pitched and hence, its distribution is quite simple. The induced voltage at the winding terminals is relatively low compared with that of the conventional BELMs with the distributed windings. From the difference of their inverter voltage ratings, the d-q axis current control BELM is competitive on the inverter cost nevertheless the number of inverters is much. In addition, the end coil length is also shorter and hence, it is superior as the rotor shaft length can be short, particularly in the two-unit tandem configuration of BELM. 2)The control method is similar to that of the interior permanent magnet synchronous motor (IPMSM), i.e., in the d-q axis current control BELM, the rotational torque is controlled by the q-axis current and the suspension force is controlled by the d-axis current (the

field-weakening or field-strengthening controls). Thus, the control method is also quite simple and the general-use 3-phase inverter can be employed to control the torque and suspension force.

The authors have proposed the d-q axis current control BELM and introduced the motor structure, the principle of torque and suspension force generation and the control method. The validity of the proposed control method has been confirmed by the experimental test results using a prototype machine. Furthermore, the characteristic of torque and suspension force have been derived based on Finite Element (FE) analysis using a simulation software. It has been made clear that it is absolutely superior compared with those of the conventional BELMs. However, the motor characteristics, for example, efficiency, losses, and the comparison and estimation with the conventional BELMs have not yet made clear.

In this paper, the losses of d-q axis current control BELM are calculated by FE analysis. The stator and rotor iron losses, eddy current loss in the rotor permanent magnets are simulated. The copper loss in the stator windings is calculated by an original method. The motor efficiency is estimated based on these computed losses and the motor output power. Furthermore, the efficiency and losses of the conventional BELMs, which two kinds of windings for motor drive and magnetic suspension are wound in a stator core, are also derived by the same method. Based on the computed results, the efficiency and losses in the d-q axis current control BELM are compared with those of the conventional BELMs, respectively, and it is discussed in detail by what the difference of losses between the BELM types is mainly caused.

2. Structure and principle of d-q axis current control bearingless motor

2.1 Motor structure

Figure 1 shows the cross section of the proposed d-q axis current control BELM. As there is only one stator winding wound on one stator core, the structure of the d-q axis current control BELM is simple and also the winding arrangement looks like conventional blushless dc motor. The stator core is classified into three sections as the section-α, the section-β and the section-γ. In the section-α, the three-phase three-wire windings $N_{u\alpha}$, $N_{v\alpha}$ and $N_{w\alpha}$ are wound; in the section-β, $N_{u\beta}$, $N_{v\beta}$ and $N_{w\beta}$ are wound; in the section-γ, $N_{u\gamma}$, $N_{v\gamma}$ and $N_{w\gamma}$ are wound. All these windings are short pitch and simple. Each section is independently controlled by separate general-use 3-phase inverters. Totally, three 3-phase inverters are needed to drive the proposed BELM. The number of inverters is more than that of the conventional BELMs. However, the capacity per an inverter may be decreased to 1/3 times that for the motor drive in the conventional BELM, and particularly the voltage rating of inverter is lower. Thus, the d-q axis current control BELM is competitive on the inverter cost.

2.2 Principle suspension force generation

The suspension force is regulated to suspend the rotor of BELM. Figure 2 shows the principle of the suspension force generation in the proposed d-q axis current control BELM. The suspension force is generated by unbalanced flux density in air-gap with controlled d-axis currents $i_{d\alpha}$, $i_{d\beta}$ and $i_{d\gamma}$ in each section. For example, in section-α the field-strengthening control is done and then the air-gap flux density is increased; in the section-β and section-γ the field-weakening control is done and then the air-gap flux density is decreased. By the net vector sum in three sections, thus the suspension force is generated in the x-positive direction. By these controlled d-axis currents, the suspension force can be successfully generated in the arbitrary radial direction.

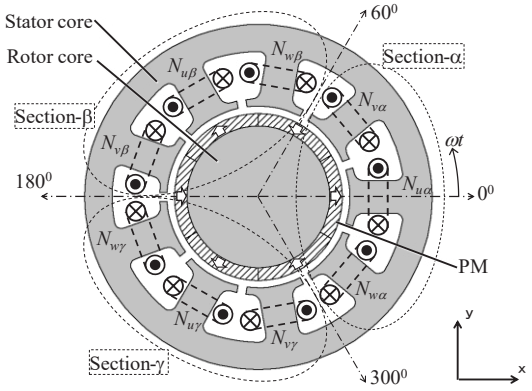

Fig. 1. Cross section of a d-q axis current control bearingless motor.

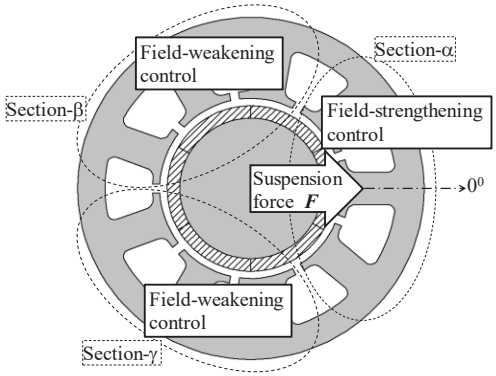

Fig. 2. Principle of suspension force generation.

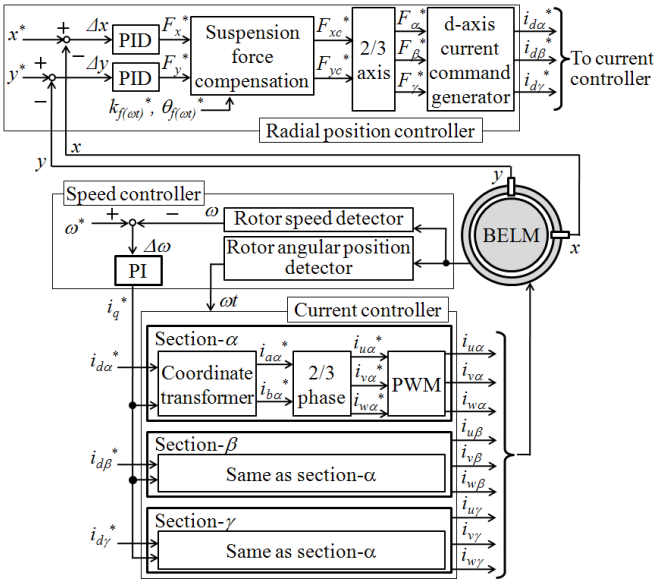

Fig. 3. Control system of d-q axis current control BELM.

2.3 Control system configuration

Figure 3 shows the control system configuration of the d-q axis current control BELM. In the motor controller, the rotor speed control method is the same as the field oriented control of the conventional ac motors. The difference $\Delta\omega$ between the detected rotor speed ω and command speed ω^* is input to the proportional-integral (PI) controller, and q-axis current command i_q^* is output of the PI speed controller which is the input to the current controllers.

In the radial position controller, the detected rotor positions x and y on the x- and y- axes with eddy-current type gap sensors are input. The differences Δx and Δy between the detected rotor positions x, y and the commands x^*, y^* are input to the proportional-integral-derivative (PID) controller, and the suspension force commands F_x^* and F_y^* in the x- and y- axes coordinate are determined. In the block of suspension force compensation, F_x^* and F_y^* are significantly compensated. Because the magnitude and direction of suspension force are undesirably varied depending on the rotor angular position due to the rotation of d-axis direction. Hence, the authors have proposed the compensation method of the suspension force to stably support the rotor shaft. We have confirmed by the simulation and experimental test results that the suspension force is correctly compensated and the stable rotor levitation is realized as shown in References. These commands F_{xc}^* and F_{yc}^* are transformed into F_α^*, F_β^* and F_γ^* in the α-, β- and γ- axes coordinate. Then, the d-axis current commands $i_{d\alpha}^*$, $i_{d\beta}^*$ and $i_{d\gamma}^*$ are determined to be proportional to the suspension force commands, respectively.

In the current controller, the current is independently controlled in each section. In the section-α, for example, the current commands i_q^* and $i_{d\alpha}^*$ are transformed into 2-phase the current commands $i_{a\alpha}^*$ and $i_{b\alpha}^*$ in the stationary coordinate. Then $i_{a\alpha}^*$ and $i_{b\alpha}^*$ are transformed into $i_{u\alpha}^*$, $i_{v\alpha}^*$ and $i_{w\alpha}^*$. The winding currents $i_{u\alpha}$, $i_{v\alpha}$ and $i_{w\alpha}$ are regulated to follow the current commands in the Pulse Width Modulation (PWM) block. The current controllers of the sections -β and -γ are the same as that of the section-α.

The validation of the proposed control system has been verified by the simulation results using an FE software and the experimental test results using a prototype machine.

3. Motor Efficiency and Losses

We have found the torque and suspension force characteristics in a d-q axis current control BELM (d-q BELM) and compared with those of the conventional BELMs, which two kinds of windings for the motor drive and magnetic suspension are wound in a stator. As a result, we have found that the d-q BELM is absolutely superior to the conventional BELMs at the view point of the characteristics of the torque and suspension force.

In this section, the efficiency and losses in a d-q axis current control BELM (d-q BELM) are computed by an FE analysis simulation software (JMAG Designer, Ver.11.1, 2-dimension) using a machine model, respectively. Based on

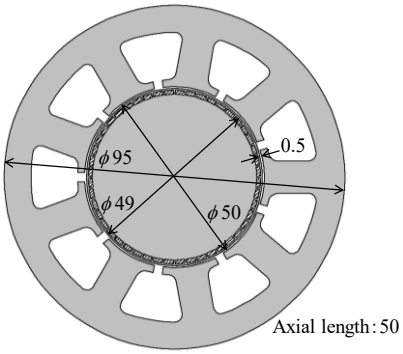

Table 1 Specification of FE model d-q axis current control BELM

Rotor core, Stator core	Silicon steel
PM	Nd-Fe-B (thickness : 1 mm)
Stator winding	146 turns/tooth, ϕ0.6 mm
Current rating	1.7 A

Fig. 4. Dimension of FE model d-q axis current control BELM.

the computed results, they are compared with those of the conventional BELMs and it is discussed in detail by what the difference of motor losses between the BELM types is caused. The combination of motor and magnetic suspension poles of the conventional BELMs is taken up to compare with the d-q BELM in this section is as follows,

- 2-pole motor and 4-pole magnetic suspension (2-4 BELM)
- 4-pole motor and 2-pole magnetic suspension (4-2 BELM)
- 6-pole motor and 4-pole magnetic suspension (6-4 BELM)

All of them above are quite same as the BELM models when the torque and suspension force characteristics were compared.

3.1 Specification of FE models

Figure 4 shows the dimension of FE model of the d-q axis current control BELM. The rotor is an interior permanent magnet type (IPM), in which the small permanent magnets are buried just below the rotor core surface. The saliency ratio is relatively low and hence, the motor performance is almost the same as that of surface-mounted permanent magnet synchronous motors (SPMSMs). The d-q axis current control BELM in Figure 4 is defined as a reference model to compare the characteristics of the torque and suspension force between the BELMs. Table 1 shows the specification of FE model of the d-q axis current control BELM.

Figures 5 (a)-(c) show the stator and rotor geometry and winding arrangement of the above conventional types of BELM. Figure 5 (a) shows that of the combination of 2-pole motor and 4-pole magnetic suspension. The inside windings N_{mu}, N_{mv} and N_{mw} in the stator slot are the 2-pole motor winding and the outside windings N_{su}, N_{sv} and N_{sw} are the 4-pole suspension winding. Two kinds of windings are wound in a stator core as described in Figure 5 (a). The rotor is 2-pole and its structure is basically the same as that of the reference model of d-q axis current control BELM in Figure 4.

Figure 5 (b) shows the cross section of the combination of 4-pole motor and 2-pole magnetic suspension. The outside windings N_{mu}, N_{mv} and N_{mw} are the 4-pole motor winding and the inside windings N_{su}, N_{sv} and N_{sw} are the 2-pole suspension winding. The rotor configurates 4-pole by the buried small permanent magnets.

Finally, Figure 5 (c) shows the cross section of the combination of 6-pole motor and 4-pole magnetic suspension. The outside windings N_{mu}, N_{mv} and N_{mw} are the 6-pole motor winding and the inside windings N_{su}, N_{sv} and N_{sw} are the 4-pole suspension winding. The rotor configurates 6-pole by the buried small permanent magnets.

The winding arrangement in all the above conventional BELM is a distributed winding. On the other hand, it is short-pitched in the d-q BELM. As mentioned above, there are significant differences between the d-q BELM and the conventional BELMs at the view points of the induced voltage at the winding terminals and the end coil length.

The FE models of the conventional BELMs are designed under the following conditions due to the comparison between the BELMs.

(1) In all the FE models, the outer diameter of the stator is the same as that of the model of d-q BELM. The rotor geometry is quite the same as that of the d-q BELM model except for the axial length.

(2) The maximum torque in the model of d-q BELM, i.e., the torque when the d-axis current is zero, is set as the reference torque. The conventional BELMs are designed by adjusting the axial length of the stator and rotor cores so that the maximum torque, i.e., the torque under the condition which there are no suspension windings and only motor winding occupies in the stator slots, is equal to the maximum torque of the d-q BELM. Therefore, the axial length of

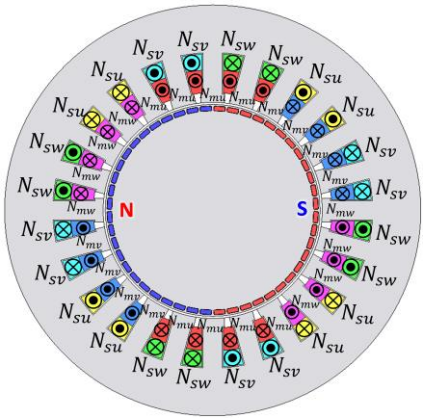

(a) 2-pole motor and 4-pole magnetic suspension (2-4 BELM).

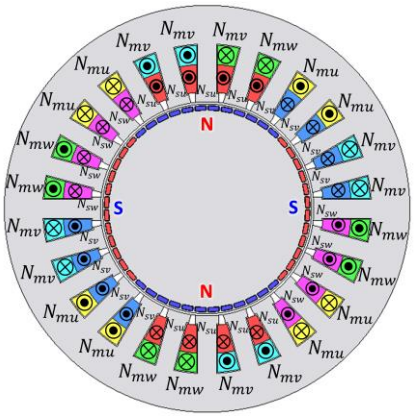

(b) 4-pole motor and 2-pole magnetic suspension (4-2 BELM).

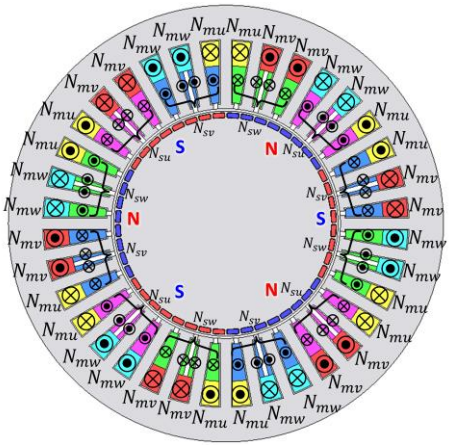

(c) 6-pole motor and 4-pole magnetic suspension (6-4 BELM).

Fig. 5. Stator and rotor geometry and winding arrangement in the conventional BELMs.

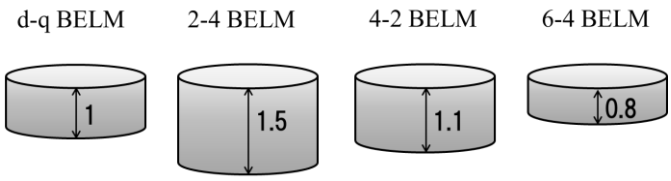

Fig. 6. Ratio of axial length in FE models.

each FE model is different. Figure 6 shows the ratio of them.

(3) The characteristics of torque and suspension force are compared under the different conditions by changing the ratio of the torque and suspension force. The winding current ratings are equal in all the FE models. In the d-q BELM, the ratio of the suspension force to the torque is regulated by changing the ratio of the d-axis current to the q-axis current. On the other hand, it is changed by adjusting the ratio of the number of suspension winding turns to that of the motor winding turns in the conventional BELMs.

(4) The flux density in the stator yoke and teeth is less than 1.6 T. Hence, the relationship between the torque and the motor current and the relationship between the suspension force and suspension current are roughly linear under this condition, respectively.

3.2 Calculation method and analysis condition

The loss in each part of the d-q axis current control BELM is computed by the FE analysis simulation software.

Table 2 Efficiency and losses in each FE model.

Model		d-q BELM	2-4 BELM	4-2 BELM	6-4 BELM
Input [W]		856	756	801	758
Iron loss [W]	stator	16.2	18.7	14.8	16.3
	rotor	1.98	0.87	2.23	1.07
Copper loss [W]		34.5	46.3	40.4	41.3
PM eddy current loss [W]		12.3	0.82	2.10	0.86
Output[W]		801	702	740	697
Efficiency [%]		92.5	91.3	92.6	92.1

The rotor and stator iron losses and PM eddy current loss are computed by FEM. Furthermore, the copper loss in the winding is calculated using the predicted overall coil length, the cross sectional area and resistivity of a coil. The machine model is the same as one, which is used for the computation of the torque and suspension force in the previous conference paper. The motor efficiency is derived based on the computed losses. In addition, the losses and efficiency of the conventional BELMs, 2-4 BELM, 4-2 BELM and 6-4 BELM in Figure 5, are also derived by the same method, respectively. The computed losses and efficiency of the d-q axis current control BELM are significantly compared with those of the conventional BELMs, respectively, and considered in detail.

3.3 Copper loss calculation

Firstly, the overall coil length is predicted to obtain the winding resistance and then, the copper loss is calculated. Figure 7 shows the approximated coil length. The center positions of conductor areas in two slots of a winding outlet and inlet are defined as the points A and B, respectively, as shown in Figure 7 (a). The line AB is set as the diameter and a half of the circle with its diameter is drawn. It means the end coil of the stator. r is the radius of the circle. l is the stack length of the stator core. Figure 7 (b) shows the cross section of a coil. The overall length L_c of this coil is as follows,

$$L_c = 2\pi r + 2l \tag{1}$$

The average length of a coil in the slot is approximated as L_c. Hence, the overall length L_s of coils in these two slots is shown as,

$$L_s = NL_c \tag{2}$$

where the number of winding turns is N in these two slots. Similarly, the coil length in the other slots is also calculated and then, one can obtain the overall coil length L_p per a phase by the amount of them. From the resistivity ρ and the area S of a coil and the L_p, the winding resistance R_p per a phase is shown as,

$$R_p = \rho \frac{L_p}{S} \tag{3}$$

From the winding resistance and current, one can obtain the copper loss.

3.4 Loss and efficiency evaluation

The copper losses in the machine models of the d-q BELM and the conventional BELMs are calculated by the equation (3), respectively. Furthermore, the iron losses in the stator and rotor and the eddy current loss in the rotor permanent magnet are computed by FE analysis software for each machine model at 4,500 r/min. These losses are summarized in Table 2. It should be noted in Table 2 that the d-axis current in the d-q BELM model and the number of suspension winding turns in the conventional BELM models are determined, respectively, so that the suspension force of about 5 times that of rotor weight is generated in each model. The winding current command is set to be sinusoidal although the current is regulated by Pulse Width Modulation (PWM) control in the inverter when the each machine will be actually operated. Hence, the iron loss caused by the current with carrier frequency component is not included in the iron losses in the stator and rotor cores and the PM eddy current loss shown in Table 2.

Figure 8 shows the stator iron loss for each BELM model. The stator iron loss of the 2-4 BELM is larger than those of the other BELMs. Because the torque of the 2-4 BELM is less than those of the other BELMs when the suspension force of 5 times that of the rotor weight is generated, as shown in the previous analyzed results. It means that the ratio of the suspension winding MMF to the motor winding MMF in the 2-4 BELM is larger than those of the other type

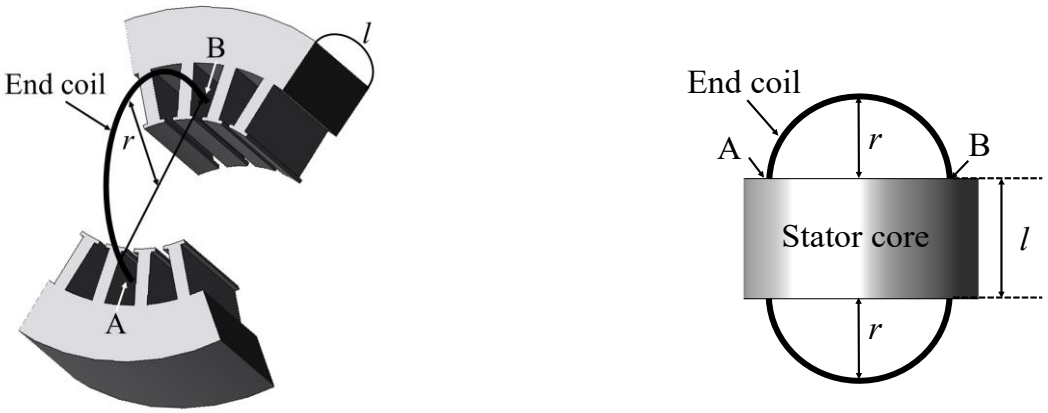

(a) End coil length. (b) Coil length per a turn.

Fig. 7. The approximated coil length.

BELMs when the suspension force of 5 times that of rotor weight is needed. It results in the longer axial length of the stator and rotor cores than those of the other BELMs to keep the same as the torque as shown in Figure 6. As a result, the stator iron loss of the 2-4 BELM is larger than the other BELMs.

Figure 9 shows the rotor iron loss for each BELM model. The rotor iron loss is quite small compared with the stator iron loss. The rotor iron loss of the 4-2 BELM is larger than that of the 2-4 BELM. The reason why it is larger is as follow: the rotational frequency of the 4-pole suspension flux is 1/2 times that of the rotor rotational frequency f [Hz]. Because the current with the same frequency component f as the 2-pole motor winding current flows in the 4-pole suspension winding in accordance with the principle of BELM. Therefore, the rotational frequency of the 4-pole suspension flux is f/2 [Hz]. On the other hand, in the 4-2 BELM, the rotational frequency of the 2-pole suspension flux is 2 times that of the rotor rotational frequency f [Hz]. Because the frequency component of the 2-pole suspension winding current is equal to that of the 4-pole motor winding current. Therefore, it is 2f [Hz]. The significant difference between the rotor iron losses in the 4-2 BELM and 2-4 BELM is caused by the difference of the suspension flux frequency.

Figure 10 shows the copper loss. The copper loss in the d-q BELM is less than those of the conventional BELMs. Because there is only one kind of winding in the stator in the d-q BELM. On the other hand, two kinds of windings, the motor winding and suspension winding, are in the conventional BELMs.

Figure 11 shows the eddy current loss of permanent magnet. The eddy current loss of permanent magnet in the d-q BELM is quite larger than those of the conventional BELMs. The reason why it is larger is as follows: The stator winding is concentrated, and it is short-pitched in the d-q BELM as shown in Figure 1. On the other hand, the winding is distributed in the conventional BELMs as shown in Figure 5. Therefore, more high frequency space harmonics are included in the stator winding MMF distribution of the d-q BELM than those of the conventional BELMs. As a result, the eddy current loss of permanent magnet in the d-q BELM is quite much.

Based on the losses shown in Figures 8-11 and the output power of the BELM, the efficiency is estimated. It is summarized in Table II. In the d-q BELM, the eddy current loss of permanent magnet is larger than those of the conventional BELMs. However, the winding copper loss is less than the others. Hence, consequently the estimated efficiency of the d-q BELM is almost the same as those of conventional BELMs.

5. Conclusion

The motor characteristics of a d-q axis current control BELM has been found by the FE model calculation. The losses in each part of the d-q BELM are simulated by FE analysis software and the efficiency is estimated based on the computed output power and losses. The efficiency and losses in the conventional BELMs are also derived and compared with those of the d-q BELM, respectively. It is discussed in detail by what the difference of losses between the BELM types is mainly caused. There is no difference on the view point of the efficiency although it is different in each loss in the d-q BELM and the others.

In the next step, the characteristic of torque and suspension force of the d-q BELM and the motor efficiency will be compared with several types of the conventional BELMs except for 3 conventional BELMs mentioned in this paper.

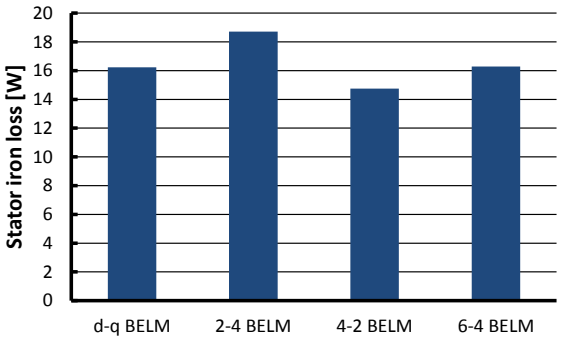

Figure 8. Stator iron loss.

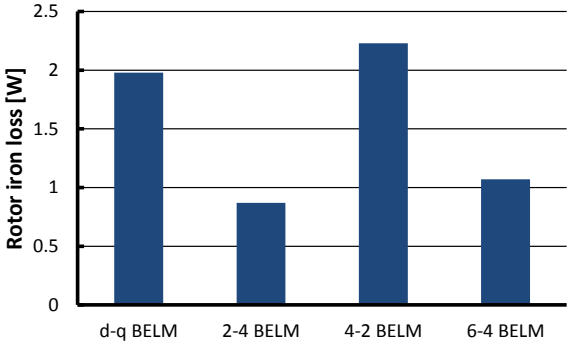

Figure 9. Rotor iron loss.

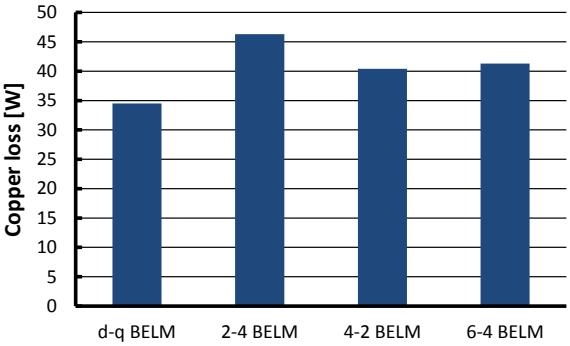

Figure 10. Copper loss.

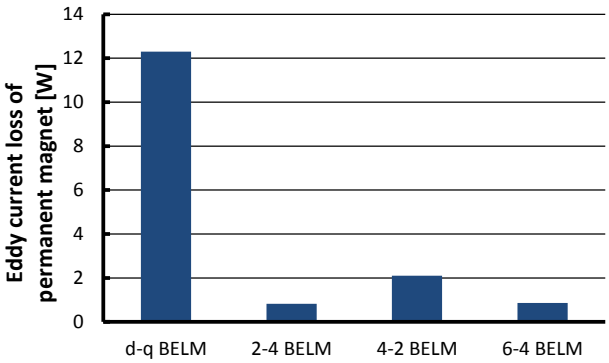

Figure 11. Eddy current loss of permanent magnet.

Furthermore, it will be compared under the other conditions, for example, under the constant stack length of the stator and rotor cores. Based on the analyzed torque and suspension force and the estimated motor efficiency, it will be discussed in detail and made clear which type of the BELMs is more superior.

References

A. Chiba, T. Fukao, O. Ichikawa, M. Ooshima, M. Takemoto and David G. Dorrell, "Magnetic Bearings and Bearingless Drives", Newnes Publishers, ISBN 0-7506-5727-8, March 2005

H. Grabner, S. Silber and W. Amrhein, "Feedback control of a novel bearingless torque motor using an extended FOC method for PMSMs", 2013 IEEE International Conference on Industrial Technology (ICIT), pp.325-330, 2013.

S. Silber, W. Amrhein, P. Bosch, R. Schob and N. Barletta, "Design aspects of bearingless slice motor", IEEE/ASME Transactions on Mechatronics, Volume 10, Issue 6, pp. 611-617, 2005.

Andreas Binder and Gabriel Munreanu, "Bearingless PM Levitation Systems" *Proceedings of the 20 12 International Conference on Electrical Machines and Systems*, Special Lecture SL-4, @Sapporo, CDROM, 2012.

Eric Severson, Robert Nilssen, Tore Undeland and Ned Mohan, "Dual Purpose No Voltage Winding Design for the Bearingless Ac Homopolar and Consequent Pole Motors", *Proceedings of the International Power Electronics Conference* (IPEC-Hiroshima 2014) *–ECCE Asia–*, pp.1412-1419, @Hiroshima, 2014.5

Hiroya Sugimoto, "Novel Single-Drive Bearimgless Motor with Wide Magnetic Gap and High Passive Stiffness", *IEEE Power and Energy Society 2014 General Meeting*, Panel Session, PESGM2014-002609, @Washington DC, 2014.7

Nobuyuki Kurita, Takeo Ishikawa, Hiromu Takada and Genri Suzuki, "Proposal of a Permanent Magnet Hybrid Type Axial Magnetically Levitated Motor", *Proceedings of the International Power Electronics Conference* (IPEC-Hiroshima 2014) *–ECCE Asia–*, pp.1697-1700, @Hiroshima, 2014.5.

Syunsuke Kobayashi, Masahide Ooshima and M. Nasir Uddin, "A Radial Position Control Method of Bearingless Motor Based on d-q Axis Current Control", *IEEE Transactions on Industry Applications*, vol.49, No.4, pp.1827-1835, 2013.

Masahide Ooshima and Yoshito Kumakura, "Stabilized Suspension Control Considering Armature Reaction in a d-q Axis Current Control Bearingless Motor", *Proceedings of the International Power Electronics Conference* (IPEC-Hiroshima 2014) *–ECCE Asia–*, pp.1715-1720, @Hiroshima, 2014.5.